

# The Significance of Early Bronze Age Iron Objects from Kaman-Kalehöyük, Turkey

*Hideo AKANUMA*

*Iwate*

## 1. INTRODUCTION

Between 1994 and 2007, five iron objects found in structures dating to the Assyrian Colony Period (20<sup>th</sup> to 18<sup>th</sup> c. B.C.) at Kaman-Kalehöyük, Turkey, were analyzed by the author (Akanuma 2002; 2003; 2007). Archaeological and archaeometallurgical analysis revealed that four of the objects were manufactured items and one was a lump of iron slag. Among the four manufactured iron fragments, three were made of steel with an estimated carbon content of 0.1 to 0.3 mass%. The microstructure of the lump of iron slag indicated that it solidified after being in a state where partially or completely melted slag was in contact with metallic iron (Akanuma 2007).

These archaeometallurgical results appear to indicate that during the Middle Bronze Age (Stratum III) at Kaman-Kalehöyük, iron objects with the composition of steel were being used in daily life and some kind of iron production activity was taking place. Evidence shows that the pre-Hittite residents (the so-called “proto-Hittites”) at Kaman-Kalehöyük had adopted some aspects of the advanced culture of Mesopotamia. Excavations yielded objects in Stratum IIIc with Mesopotamian characteristics such as red polished earthenware (Omura 2004). Other archaeological evidence, such as the many objects from Mesopotamia discovered at the site of Kültepe (Özgüç 1986), indicates that Central Anatolia had strong commercial links with Mesopotamia. Therefore, it is possible that iron objects or iron production techniques were brought to Anatolia from Mesopotamia by the Assyrians or another people.

In 2007, iron objects excavated in previous years from Stratum IIIc and Stratum IVa (Early Bronze Age) at Kaman-Kalehöyük were examined by the author. Twenty-one objects were selected for

archaeometallurgical analysis and brought to the Iwate Prefectural Museum laboratory, Japan. Analysis of four objects from Stratum IVa (22<sup>nd</sup> to 20<sup>th</sup> c. B.C.) was recently completed and it was found that one of the objects was an iron fragment with the composition of steel. The other three objects were a lump of iron ore and two lumps of a partially or completely melted clay-like substance. These results raise the possibility that iron production methods had already been established during the Early Bronze Age. This paper discusses the archaeometallurgical analysis of these four objects. Research on the other 17 objects is not yet complete.

## 2. OBJECTS ANALYZED

Sample No.1 (Fig. 1a<sub>1</sub>) is a bar-shaped object with weak magnetism, whose surface is covered by brown soil. As described below, an X-ray photograph revealed that this is a piece of a manufactured iron object. Sample No.2 (Fig. 2a<sub>1</sub>) is a red-brown lump of iron ore. Samples No.3 (Fig. 3a<sub>1</sub>) and No.4 (Fig. 4a<sub>1,2</sub>) are composed of a partially or completely melted clay-like substance whose color is grayish brown. A reddish brown area is also observed on a part of the surface of Sample No.3. Fine white grains are contained in Sample No.4. They are believed to be related to iron or copper production.

Table 1 lists the archaeological provenance data for each object. These four samples were discovered from three different layers composed of burned soil according to Dr. Sachihiko Omura, director of the Kaman-Kalehöyük excavation. The Early Bronze Age date of the objects is based on stratigraphic evidence and the typology of pottery excavated with the objects. Radiocarbon dating was performed on pieces of charred grains from the layer above that in which Sample No.2

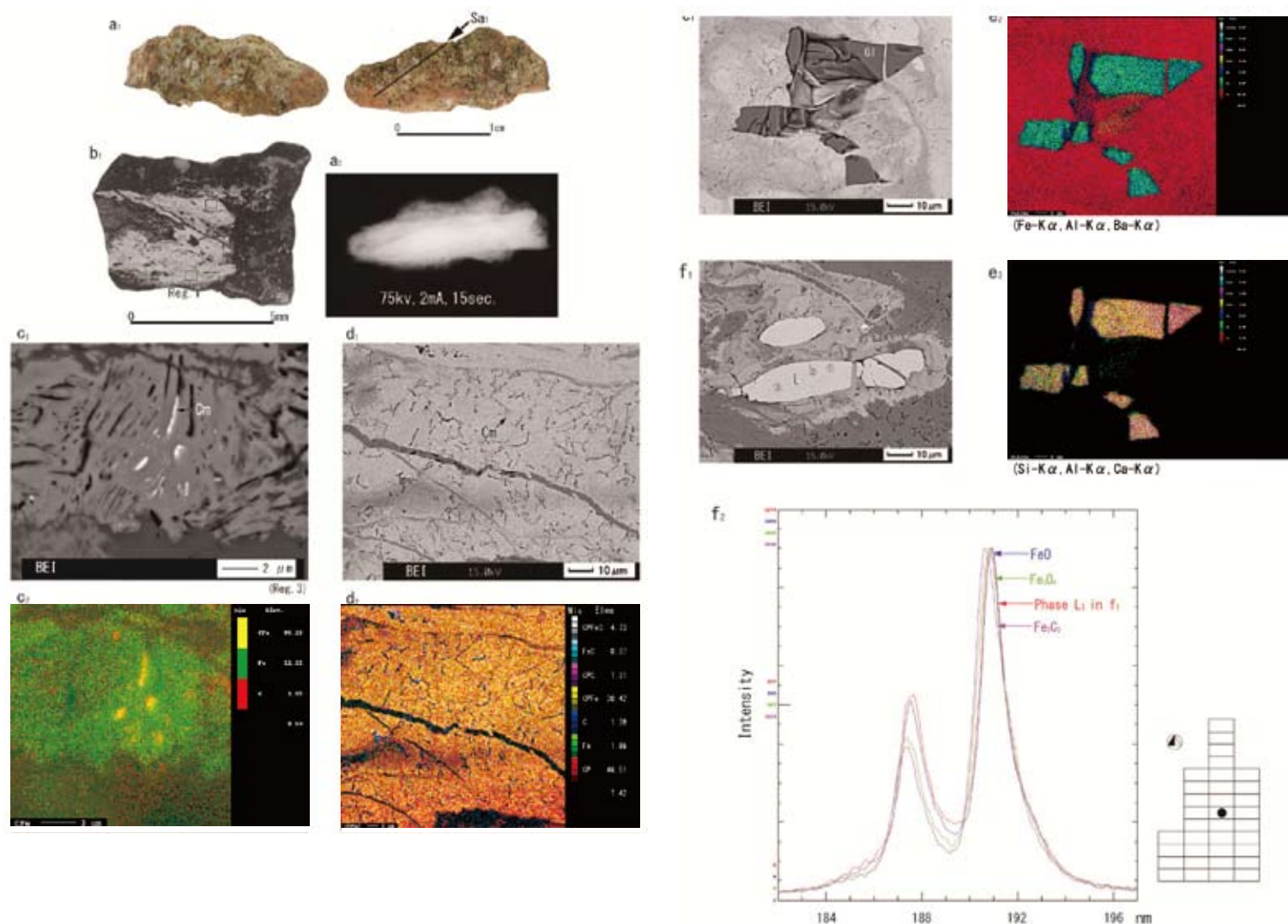


Fig. 1 Metallographic analysis of Sample No.1. a: External appearance. The metallographic sample was extracted from the marked location. a<sub>2</sub>: X-ray photograph. b<sub>1</sub>: Macrostructure. c<sub>1</sub> and c<sub>2</sub>: Backscattered electron (BE) image and a combined X-ray color-map of Fe-K $\alpha$  and C-K $\alpha$  within the area (Reg.1) in b<sub>1</sub>. Cm: Cementite or its holes. d<sub>1</sub> and d<sub>2</sub>: BE image and pseudo full-color map of d<sub>1</sub>. Blue colored areas correspond to the area composed of cementite or its holes. e<sub>1</sub>-e<sub>3</sub>: BE image and combined X-ray colormaps of Fe-K $\alpha$ , Al-K $\alpha$ , and Ba-K $\alpha$ , and Si-K $\alpha$ , Al-K $\alpha$ , and Ca-K $\alpha$ , respectively. f<sub>1</sub> and f<sub>2</sub>: Fe-L $\alpha$  and Fe-L $\beta$  spectra of three Fe standard samples (FeO, Fe<sub>3</sub>O<sub>4</sub>, and Fe<sub>2</sub>O<sub>3</sub>), and phase L<sub>1</sub> in f<sub>1</sub> by EPMA. The predominant constituent of phase L<sub>1</sub> is believed to be wüstite. (Excavation plan from Omura 2005)

was discovered and also on pieces of charcoal from just above where from Samples No.1 and No.3 were found. The C-14 date of the charred grains is 2200 to 2030 cal B.C. (Omori and Nakamura 2007) and that of the charcoal is 2120 to 2030 cal B.C. (Atsumi *et al.* 2008). These results corroborate the archaeological dating very well. According to Dr. Sachihiko Omura, there is little possibility that these objects dropped from an upper

layer, as the surface of Stratum IVa is covered by a thick layer of burned soil.

### 3. SAMPLE PREPARATION

Samples of approximately 200–300 mg were taken from Sample No.1, and of approximately 2000 mg from

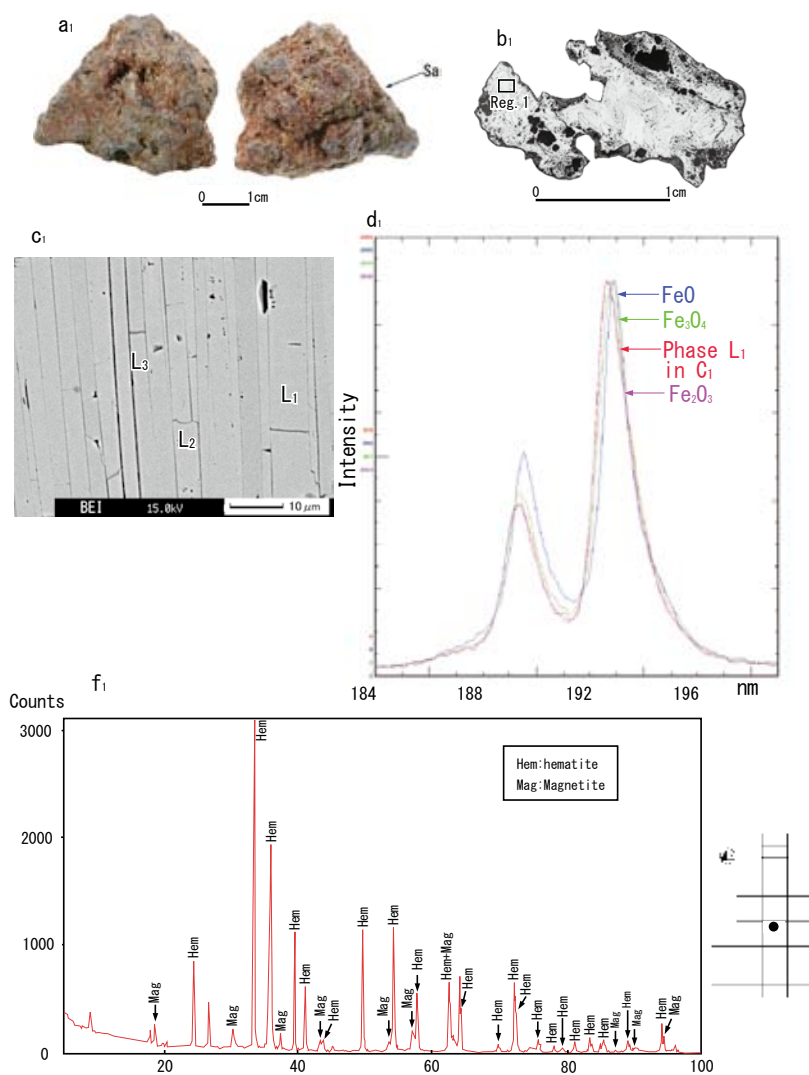


Fig. 2 Metallographic analysis of Sample No.2. a<sub>1</sub>: External appearance. The metallographic sample was extracted from the marked location. b<sub>1</sub>: Macrostructure. c<sub>1</sub>: BE image of the area (Reg.1) in b<sub>1</sub>. d<sub>1</sub>: Fe-L $\alpha$  and Fe-L $\beta$  spectra of three Fe standard samples (FeO, Fe<sub>3</sub>O<sub>4</sub>, and Fe<sub>2</sub>O<sub>3</sub>), and phase L<sub>1</sub> in c<sub>1</sub> by EPMA. f<sub>1</sub>: XRD pattern. The predominant constituent of phase L<sub>1</sub> is hematite. (Excavation plan from Omura 2005)

Samples No.2, No.3 and No.4. Samples were taken using a portable drill equipped with a diamond cutting wheel. V-shaped cuts were put in Samples No.2, No.3 and No.4, and then samples for analysis were extracted from them. The extracted samples from Samples No.1, No.3 and No.4 were divided into two parts: the larger portions from Samples No.1 and No.3 were used for metallographic examination, and the larger portion from Sample No.4 was used for examination with a polarizing microscope. The smaller portions from these three samples were used for chemical analysis. The extracted sample from Sample No.2 was divided into three parts. One was crushed and ground into a fine powder for X-ray powder diffraction analysis (XRD). The other two were devoted to metallographic examination and chemical analysis.

Because the surface of Sample No.1 was covered with a great deal of soil, a sample for chemical analysis was extracted from the surface in addition to the inner portion, in order to consider the influence of contamination from the burial deposits. (The surface sample, indicated by Suf, is composed mainly of soil and contains a small amount of corrosion products).

#### 4. ANALYTICAL METHODS

The samples for metallographic examination were sectioned, mounted with epoxy resin, ground with emery paper, and

Table 1 Examined objects from Stratum IVa

No.	Object	Description of Excavation						Year Number	Stratum
		Sector	Grid	Date	Provisional Layer	Structure			
1	Iron fragment	North	IV	XXXIX-54	010831	(73)-c	-	01000854	IVa
2	Iron ore	North	IV	XXXVIII-55	020708	(81)	-	02000824	IVa
3	Fragment of furnace wall (Hearth frag)	North	IV	XXXVIII-55	010815	(73)	-	01000853	IVa
4	Fragment of furnace wall (Hearth frag)	North	IV	XXXVIII-54	020702	(60)	-	02000825	IVa

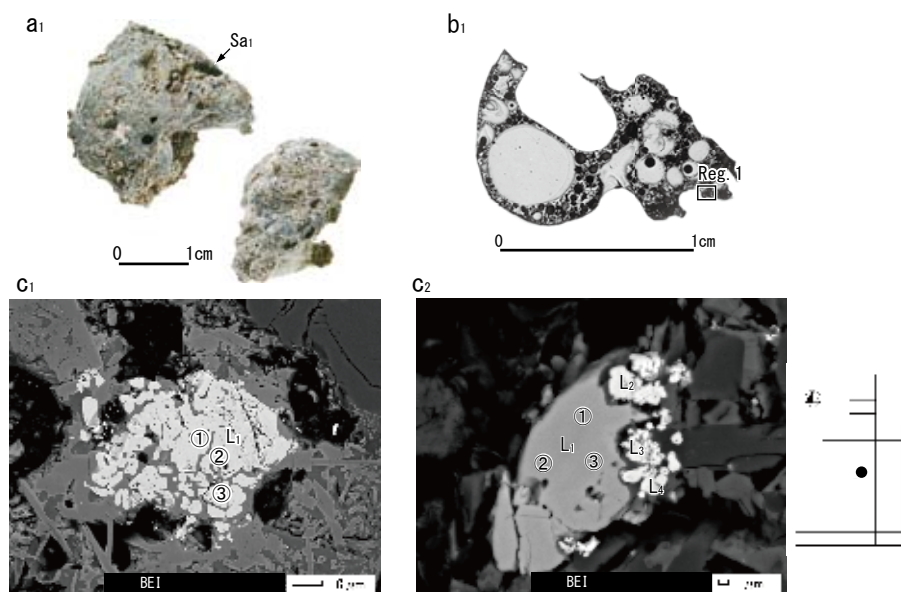


Fig. 3 Metallographic analysis of Sample No.3. a<sub>1</sub>: External appearance. The metallographic sample was extracted from the marked location. b<sub>1</sub>: Macrostructure. c<sub>1</sub> and d<sub>1</sub>: BE images of the area (Reg.1) in b<sub>1</sub>. (Excavation plan from Omura 2005)

then polished using diamond paste. The prepared samples were then examined under an optical microscope. Electron probe microanalyses (EPMA) were then performed with a JEOL JXA 8100 equipped with three wavelength-dispersing X-ray spectrometers, in order to examine the microstructure and to identify the mineral

phase compositions in the non-metallic inclusions of Sample No.1, and the mineral phases in Samples No.2, No.3, and No.4.

XRD was recorded by a JEOL JDX-3532 under the following conditions: Cu-K $\alpha$  radiation at 40kV and 30mA, divergence slit, scatter slit=1 $^\circ$ , receiving slit =0.2mm, 2 $\theta$ =5-85 $^\circ$ .

Inductively coupled plasma optical emission spectroscopy (ICP-OES), using a PERKIN ELMER Optima 4300DV, was employed for the chemical analysis of twenty elements from each sample (including both the inner sample and the surface sample from No.1); the results are in Tables 2, 5, and 6. The elements determined, and the analytical lines selected (nm), were as follows: Fe (239. 562), Cu (324. 752), Ni (231. 604), Co (228. 616), Mn (257. 610), P (213. 617), Ba (233. 527), Ti (334. 940), Si (251. 611), Ca (317. 933), Al (396. 153), Mg (285. 213), V (290. 880), Sb (206. 836), As (193. 696), Mo (202. 031), Cr (284. 325), Zr (343. 823), Y (371. 029) and S (181. 975). The analytical procedures and operating conditions used here were the same as described in Akanuma (2007).

Table 2 Chemical composition of Sample No.1 by ICP-OES

Sub.No	T.Fe	Cu	Ni	Co	Mn	P	Ba	Ti	Si	Ca	Al	Mg	V	Sb	As	Mo	Cr	Zr	Y	S	m.s.	n.m.i
Sa <sub>1</sub>	63.85	0.020	0.002	0.001	0.017	0.12	0.067	0.343	2.51	0.555	0.992	0.145	0.024	<0.01	0.01	<0.001	-	<0.001	<0.001	0.02	Cm(0.1-0.3)	Gl,Wus
Suf	15.94	0.004	0.002	0.002	0.025	0.18	0.007	0.375	15.5	1.62	1.85	0.236	0.054	<0.01	0.03	<0.001	-	<0.001	<0.001	0.04	-	-

Suf=sample extracted from the outer surface of Sample No.1

Sa<sub>1</sub>=sample extracted from the inner portion of Sample No.1

Cm=cementite or its holes ;the number in a parenthesis is a carbon content estimated from a microstructure

m.s.=microstructure

n.m.i=non-metallic inclusions. Gl=glassy silicate, Wus=wüstite

Table 3 Results of quantitative analysis of mineral compounds found in Samples No.1-No.3 by EPMA

No.	Spot		chemical components (mass %)							total	
			Fe	Mg	Mn	Al	Ti	Ca	O		
1	Fig.1f <sub>1</sub>	L <sub>1</sub>	①	72.8	0.94	3.04	0.23	-	-	22.6	99.64
			②	72.9	0.99	3.03	0.23	-	-	22.5	99.70
			③	72.9	1.01	3.13	0.23	-	-	22.6	99.85
2	Fig.2c <sub>1</sub>	L <sub>1</sub>	-	69.7	-	-	0.08	0.20	-	28.8	98.73
		L <sub>2</sub>	-	69.4	-	-	0.15	0.22	-	28.6	98.32
		L <sub>3</sub>	-	68.8	-	-	0.10	0.89	-	28.5	98.33
3	Fig.3c <sub>1</sub>	L <sub>1</sub>	①	69.0	0.63	0.16	0.81	0.12	0.14	25.1	95.99
			②	68.7	0.67	0.16	0.82	0.16	0.16	25.2	95.94
			③	68.4	0.34	0.16	1.24	0.29	0.20	25.5	96.10

The numbers refer to sample descriptions in Table 1.

One portion from Sample No.4 was examined with a polarizing microscope in order to determine its main constituent minerals. This was performed by Dr. Nobutaka Tsuchiya, professor of geology at Iwate University, Faculty of Education.

## 5. ANALYTICAL RESULTS

### 5.1 Chemical composition of Sample No.1

Table 2 reports the analytical data obtained by ICP-OES. The total iron (T.Fe) content of Sample No.1Sa<sub>1</sub> (inner sample) is 63.85 mass%, indicating that this sample is chiefly composed of iron corrosion. The Cu content is 0.020 mass%, Ni 0.002 mass%, Co 0.001 mass% and Ba 0.067 mass%. The surface sample extracted from No.1 (No.1Suf), which consists primarily of soil and corrosion products, has 15.94 mass% of T.Fe, 0.004 mass% of Cu, 0.002 mass% of Ni, 0.002 mass% of Co and 0.007 mass% of Ba.

As discussed in a previous paper (Akanuma 2005), the elements Cu, Ni and Co are believed to remain in the iron metal throughout the process of smelting, refining, and forging. These three elements, therefore, can be diagnostic in classifying iron artifacts by composition, if there is little contamination by these same elements in the surrounding burial deposits. In this analysis, the Cu content in Sample No.1Suf is lower than in Sample No.1Sa<sub>1</sub>, indicating that the Cu content originated from the object itself, specifically from the raw iron materials used to produce it. The Ni and Co contents in both the surface and inner samples are equal to or less than 0.002 mass%. Even if there was some contamination from burial, it is believed to be negligible. Therefore, we can conjecture that the raw iron materials used to make

object No.1 contained minor amounts of Ni and Co.

Another notable observation is the Ba content, which is lower in Sample No.1Suf than in Sample No.1Sa<sub>1</sub>, indicating it originated from the object itself. Ba content is noted again in the discussions below.

### 5.2 Metallographic examination of Sample No.1

Sample No.1, a bar-like object (Fig. 1a<sub>1</sub>), was covered with soil and corrosion products as shown in an X-ray photograph (Fig. 1a<sub>2</sub>). The cross section of this object is rectangular, indicating it was manufactured. The cross section is almost completely composed of corrosion (Fig. 1b<sub>1</sub>). There are many voids and cracks in the structure.

In the EPMA backscattered electron (BE) image of the area (Reg.1) in that cross section, fine white crystals (Cm) with a metallic luster and fine dark structures are observed (Fig. 1c<sub>1</sub>). The EPMA combined X-ray color-map reveals that the main components of these white crystals are Fe and C (Fig. 1c<sub>2</sub>). The fine dark structures are identified as holes formed by the loss of the fine crystals based on a secondary electron image and a topographic image. Considering that these fine crystals and dark structures form lamellar structures, we believe that the fine crystals are cementite (Fe<sub>3</sub>C). A similar structure was found in iron fragments dating to the Assyrian Colony Period at Kaman-Kalehöyük (Akanuma 2002 and 2003). Fig.1d<sub>1</sub> is the EPMA backscattered electron image of the area (Reg.2) in Fig. 1b<sub>1</sub>. Island-shaped regions composed of lamellar structures are observed throughout the whole region of this image. In Fig.1d<sub>2</sub>, the lamellar structures composed of cementite and its holes correspond to the blue colored region. The estimated carbon content of this structure is 0.1 to 0.3 mass%, based on the area ratio occupied by these lamellar structures shown in Fig. 1d<sub>1</sub> and Fig. 1d<sub>2</sub>.

Table 4 Results of quantitative analysis of mineral compounds found in Sample No.3 by EPMA

Spot		chemical components (mass %)									total	
		SiO <sub>2</sub>	CaO	Y <sub>2</sub> O <sub>3</sub>	UO <sub>2</sub>	ZrO <sub>2</sub>	HfO <sub>2</sub>	FeO	Al <sub>2</sub> O <sub>3</sub>	TiO <sub>2</sub>		
Fig.3c <sub>2</sub>	L <sub>1</sub>	①	34.2	0.10	0.10	0.07	64.8	1.51	0.20	-	-	100.97
		②	33.8	0.10	0.69	0.35	63.9	0.87	0.18	-	-	99.87
		③	34.1	0.11	0.54	0.29	64.4	0.98	0.17	-	-	100.64
	L <sub>2</sub>	-	2.46	3.31	-	0.27	89.3	1.71	1.19	0.52	0.33	99.08
	L <sub>3</sub>	-	4.94	2.96	-	0.54	83.7	1.44	1.80	1.18	0.50	97.07
L <sub>4</sub>	-	2.04	1.17	-	0.35	92.7	1.63	1.43	0.51	0.35	100.20	

Non-metallic inclusions consisting of a dark area (G1) and a light gray and granular area ( $L_1$ ) are seen in Figs.1e<sub>1</sub> and 1f<sub>1</sub>. According to semi-qualitative EPMA analysis and the combined X-ray color-map (Figs.1e<sub>2</sub> and 1e<sub>3</sub>), the area (G1) is a glassy silicate of a FeO-CaO-Al<sub>2</sub>O<sub>3</sub>-K<sub>2</sub>O-MgO-BaO-MnO-SiO<sub>2</sub> system; the semi-quantitative analysis reveals that there is more than 3 mass% BaO in this inclusion. Fig.1f<sub>2</sub> shows the Fe-L $\alpha$  and Fe-L $\beta$  spectra of three Fe standard samples (FeO, Fe<sub>3</sub>O<sub>4</sub> and Fe<sub>2</sub>O<sub>3</sub>), and phase  $L_1$  in Fig.1f<sub>1</sub>. The Spectral Shape of Fe-L of phase  $L_1$  is almost the same as that of FeO. Considering the result of the quantitative EPMA analysis seen in Table 3, the predominant constituent of phase  $L_1$  is believed to be wüstite.

5.3 Chemical composition of Samples No.2, No.3 and No.4

Sample No.2 (Fig. 2a<sub>1</sub>), described below as being composed mainly of hematite, has 67.58 mass% of T.Fe, 0.61 mass% of Si, 0.214 mass% of Ba and 0.05 mass% of S. The Ba and S contents should originate from the gangue mineral in this sample. A major component of Sample No.2 is Fe (Table 5).

Major components of Samples No.3 and No.4 are Si and Al. The T. Fe contents of these two samples are only 3.65 mass% and 3.48 mass%, respectively. This is consistent with the naked eye examination of these samples. Sample No.3 has 0.081 mass% Ba and No.4 has 0.112 mass% Ba (Table 6).

5.4 Metallographic and mineralogical examination of Samples No.2, No.3 and No.4

Fig. 2b<sub>1</sub> shows the macrostructure of Sample No.2. This sample has weak magnetism. A gray phase forming

a layered structure is observed in the BE image (Fig. 2c<sub>1</sub>). According to quantitative EPMA analysis (Table 3), the gray phase ( $L_1$ ,  $L_2$ , and  $L_3$  in Fig. 3c<sub>1</sub>) is chiefly composed of iron oxide. This chemical composition almost coincides with that of hematite (Fe<sub>2</sub>O<sub>3</sub>). According to the Fe-L $\alpha$  and Fe-L $\beta$  spectra of three Fe standard samples (FeO, Fe<sub>3</sub>O<sub>4</sub> and Fe<sub>2</sub>O<sub>3</sub>) shown in Fig. 2d<sub>1</sub> and phase  $L_1$  in Fig. 2c<sub>1</sub>, the Spectral Shape of Fe-L of phase  $L_1$  is almost the same as that of Fe<sub>2</sub>O<sub>3</sub>. The X-ray powder diffraction pattern matches that of hematite. Weak peaks belonging to magnetite are also present (Fig.2f<sub>1</sub>). This correlates with the observation of weak magnetism. This analysis indicates that the major component of Sample No.2 is hematite, with a small amount of magnetite.

Sample No.3 (Fig. 3a<sub>1</sub>) appears to be a partially or completely melted object. The macrostructure of this sample has many voids and cracks (Fig. 3b<sub>1</sub>). Gray phases and a dark gray phase are observed in the BE images (Figs. 3c<sub>1</sub> and 3c<sub>2</sub>). Based on the EPMA analysis (Tables 3 and 4), phase  $L_1$  in Fig. 3c<sub>1</sub> is believed to be magnetite, and phase  $L_1$  in Fig. 3c<sub>2</sub> has a chemical composition similar to zircon (ZrSiO<sub>4</sub>). Minute grains with metallic luster are seen in contact with phase  $L_1$  in Fig. 3c<sub>2</sub>. The predominant component of these grains ( $L_2 \sim L_4$  in Fig. 3c<sub>2</sub>) is zirconium oxide (ZrO<sub>2</sub>) (see Table 4).

Sample No.4 (Figs. 4a<sub>1</sub> and 4a<sub>2</sub>) also appears to be a partially melted object. Fig. 4b<sub>1</sub> and Fig. 4c<sub>1</sub> show photomicrographs taken using a polarizing microscope. According to Dr. Nobutaka Tsuchiya, in the vesicular structure a dark brown glassy area with fragments of quartz and fragments of granite containing quartz, potassium feldspar (Kfs), plagioclase (Pl), and hornblende (Hbl) is observed. This indicates that Sample No.4 is likely to be clay containing granitoid clastics.

Table 5 Chemical composition of Sample No.2Sa<sub>1</sub> by ICP-OES

T.Fe	Cu	Ni	Co	Mn	P	Ba	Ti	Si	Ca	Al	Mg	V	Sb	As	Mo	Cr	Zr	Y	S
67.58	0.004	0.001	<0.001	0.004	0.04	0.214	0.127	0.61	0.051	0.455	0.023	0.019	<0.01	<0.01	<0.001	0.002	<0.001	<0.001	0.05

Table 6 Chemical composition of fSamples No.3 and No.4 by ICP-OES

No.	Sub.No	T.Fe	Cu	Ni	Co	Mn	P	Ba	Ti	Si	Ca	Al	Mg	V	Sb	As	Mo	Zr	Y	S
3	Sa <sub>1</sub>	3.65	<0.001	<0.001	0.001	0.076	0.40	0.081	0.411	28.4	6.91	6.98	1.27	0.003	0.01	0.01	<0.001	0.010	<0.001	<0.01
4	Sa <sub>1</sub>	3.48	<0.001	0.001	0.001	0.066	0.07	0.112	0.391	29.0	2.08	9.04	0.782	0.001	0.01	<0.01	<0.001	0.002	<0.001	<0.01

The numbers refer to sample descriptions in Table 1.

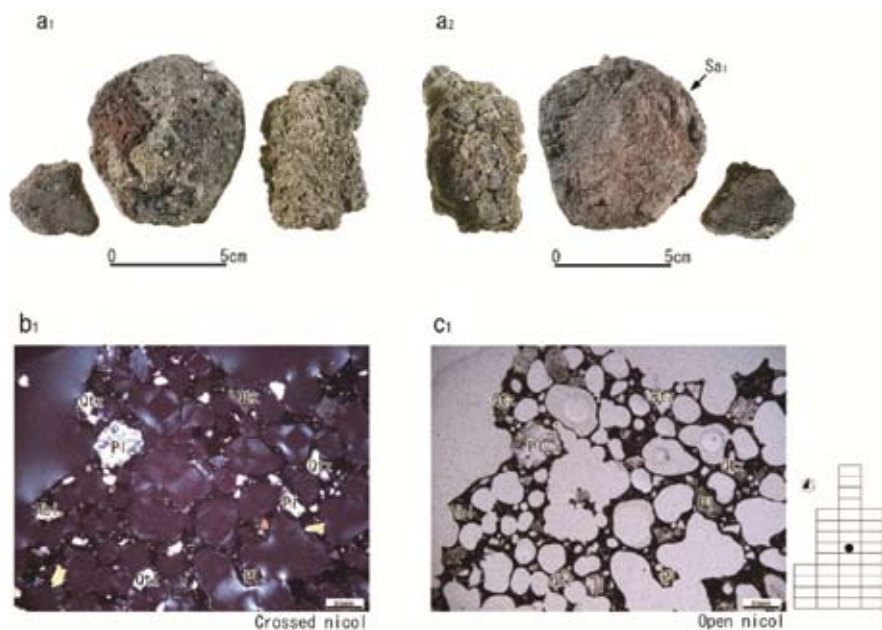


Fig. 4 Polarized microphotographs of Sample No.4. a<sub>1</sub>: External appearance. Sample was extracted from the marked location. b<sub>1</sub> and c<sub>1</sub>: Minerals observed in the extracted sample by polarized microscopy. Qtz=quartz, Kfs=potassium feldspar, Pl=plagioclase, and Hbl=hornblende. (Excavation plan from Omura 2005)

## 6. DISCUSSION

Sample No.1 is part of an iron object made of steel with a carbon content believed to be 0.1 to 0.3 mass%. This sample was discovered in a structure belonging to Stratum IVa (22<sup>nd</sup> c. B.C. to 20<sup>th</sup> c. B.C.). The combination of carbon dating, archaeological context, and archaeometallurgical examination indicates that it is likely that the use of ironware made of steel had already begun in the third millennium B.C. in Central Anatolia.

The non-metallic inclusion found in this sample is composed of a glassy silicate whose main components are FeO, CaO, SiO<sub>2</sub>, Al<sub>2</sub>O<sub>3</sub>, K<sub>2</sub>O, MgO, MnO and BaO. This is the first time that more than 3 mass% of BaO has been detected in the non-metallic inclusions of ironware from Kaman-Kalehöyük. This raises the possibility that the acquisition area of the Stratum IVa ironware was different from that of the Stratum IIIc ironware analyzed previously.

Sample No.2 is a lump of hematite. In a previous analysis (Akanuma 2002), a small lump of iron ore was found to be composed mainly of limonite and hematite,

with a small amount of chalcopyrite (Ccp: CuFeS<sub>2</sub>). These two samples are believed to have different origins because of their different mineral and chemical compositions.

Samples No.3 and No.4 are believed to be parts of production equipment or tools. In Sample No.3, minute granular regions composed of magnetite were observed, indicating that the material may have been generated by reaction with iron oxide. The petrological and mineralogical examination of Sample No.4 by Dr. Tsuchiya revealed that it is likely to have been composed of clay containing granitoid clastics. It is difficult to determine the original materials of Sample No.3, as there are no minerals or fragments of rocks to identify. The chemical compositions of the two samples are similar, so they may have been composed of almost the same materials. This matter should be clarified

by further research.

As noted above, there is evidence that the proto-Hittites at Kaman-Kalehöyük adopted the advanced culture of Mesopotamia. Therefore, we need to consider the possibility that iron objects or iron production techniques were brought from the Mesopotamian region by the Assyrians or another people, or that iron production techniques were established through cooperation between the proto-Hittites and the Assyrians, or another people. However, the discovery in a Stratum IVa structure of a piece of ironware with the composition of steel and of other iron materials that seem to relate to production raises the following possibility: the proto-Hittites developed iron production techniques independently. In order to clarify this matter, we need to find and analyze larger iron objects and other iron-related materials from Stratum IVa.

At the same time, we must continue looking for evidence of iron-related activity in Stratum IVb. According to excavation results, the influence of Mesopotamian culture in Anatolia during the cultural age of Stratum IVb was not very strong. The possibility of the independent development of iron production technology

by the proto-Hittites could be considered high if iron objects, especially ironware and iron slag, were found in Stratum IVb.

## 7. CONCLUSION

The archaeological and archaeometallurgical studies of iron objects excavated from Stratum IVa at Kaman-Kalehöyük strongly suggest that iron production had already been established during the Early Bronze Age. Further examination of iron objects excavated from all levels of Stratum IV will bring us a better understanding of the transition from bronze to iron in the Near East.

## ACKNOWLEDGEMENTS

The author is very grateful to Dr. Sachihito Omura and all the members of the Kaman-Kalehöyük excavation team for their support of this study and useful suggestions. The author also appreciates Dr. Nobutaka Tsuchiya for his polarizing microscope examinations. The author would like to thank Dr. Kimihisa Ito, Ms. Claire Peachey and Mr. Kyle Steinke for helpful comments.

## BIBLIOGRAPHY

Akanuma, H.

- 2002 "Iron Objects from the Architectural Remains of Stratum III and Stratum II at Kaman-Kalehöyük. Correlation between Composition and Archaeological Levels," AAS XI, pp. 191-200.
- 2003 "Further Archaeometallurgical Study of 2nd and 1st Millennium BC Iron Objects from Kaman-Kalehöyük, Turkey," AAS XII, pp. 142-143.
- 2005 "The Significance of the Composition of Excavated Iron Fragments from Stratum III at the Site of Kaman-Kalehöyük, Turkey," AAS XIV, pp. 147-157.
- 2007 "Analysis of Iron and Copper Production Activity in Central Anatolia during the Assyrian Colony Period," AAS XVI, pp. 125-139.

Atsumi, S., J. Yoneda, N. Shibata, and I. Nakai

- 2008 "Radiocarbon Chronology on Bronze Age at Kaman-Kalehöyük, Turkey in the Central Anatolia," *Archaeology and Natural Science*, vol. 53, pp. 37-53 (in Japanese).

Omori, T., and T. Nakamura

- 2007 "Radiocarbon Dating of Archaeological Materials Excavated at Kaman-Kalehöyük: Second Report," AAS XVI, pp. 111-123.

Omura, S.

- 2004 *Excavation in Anatolia: 20 Years of Kaman-Kalehöyük*, NHK Books pp.146-153 (in Japanese).

Özgüç, T.

- 1986 "New Observations on the Relationship of Kültepe with Southeast Anatolia and North Syria during the Third Millennium B.C.," in J. V. Canby *et al.* (eds), *Ancient Anatolia: Aspects of Change and Cultural Development*, *Wisconsin Studies in Classics*, pp. 31-47.

*Hideo Akanuma*

*Iwate Prefectural Museum*

*34 Uedamatsuyashiki, Morioka*

*Iwate 020-0102*

*Japan*

*Akanuma@iwapmus.jp*